Available online at www.sciencedirect.com

SciVerse ScienceDirect

Proceedings of the Combustion Institute 34 (2013) 2649–2656

Proceedings of the Combustion Institute

www.elsevier.com/locate/proci

Thermo-mechanical modeling of firebrand breakage on a fractal tree

B.W. Barr, O.A. Ezekoye *

Department of Mechanical Engineering, The University of Texas at Austin, 1 University Station, C2200 Austin, TX 78712-0292, USA

Available online 11 August 2012

Abstract

Firebrand lofting models rely on prescribed size distributions for brands that are available for lofting. Typically, the assumption made is that the balance between aerodynamic forces and weight defines the characteristic size of lofted brands. This work develops a model for predicting the size distribution of brands lofted from a fractal tree using simple mechanical breakage models that are coupled to a simple thermal decomposition model. The breakage model is parameterized by fuel density and strength data that are experimentally generated. Dimensionless parameters are identified to characterize the degradation and breakage processes. The breakage model is then coupled to a plume model to form a description of the breakage, transport, and mass loss of branching vegetative fuel packets in wildland fire scenarios. A Monte Carlo simulation is then performed for branching fuels in a wildland fire case study, and the presence of an optimal branch diameter for mass transport by brand lofting is identified.

Keywords: Brand lofting; Wood; Mechanical strength; Brand generation; Wildland fire

1. Introduction

The lofting of embers, or brands, from large-scale wildland fires is an important mechanism in the spread of these fires. Brand lofting and deposition may be thought of as a three-stage process. In the first stage, brands are generated from the parent fuel element by aerodynamic shearing of structurally weakened elements. In the second stage, the brands are transported upwards within the fire plume to a high elevation. In the third stage, the brands exit the plume and are carried by wind ahead of the flame front and deposited on the ground. Throughout the transport process, each brand loses mass, and depending on the type of fuel and the initial dimensions of a brand, it will either burn out in the air or survive the lofting process and land with sufficient mass and thermal energy to start a spot fire.

Because the brand transport process is a critical part of wildfire spread modeling, accurate representation of the brand lofting process is necessary in order to obtain wildfire spread models with reasonable predictive capabilities. Much analysis has been done on modeling the plume lofting and wind propagation stages of brand lofting [1–3], and significant experimental work has been done to characterize the size and number distribution of brands generated and their effects on fire spread [4,5]. Relatively little work has been done to model the generation of brands from the parent

* Corresponding author. Fax: +1 512 471 1045.
E-mail address: dezekoye@mail.utexas.edu (O.A. Ezekoye).

1540-7489/$ - see front matter © 2012 The Combustion Institute. Published by Elsevier Inc. All rights reserved.
http://dx.doi.org/10.1016/j.proci.2012.07.066

fuel package. This work primarily focuses on the brand generation process by creating a model system to analyze the breakage of brands from branching fuel structures due to interaction with a fire plume. The breakage model is then coupled to a simplified version of a plume and propagation model created by Woycheese et al. [3], and the complete model is used to predict the mass distribution and propagation distance of embers in a wildland fire case study.

2. Brand generation model

For fuels which have dendritic or branching geometries, such as wildland vegetation, body forces and shear loading produce stresses on exposed protuberances, making them susceptible to breakage. As mass loss associated with thermal degradation occurs for the protuberances, their geometry and strength properties may be changed to a point at which fracture occurs, and lofted brands are produced. The thermo-mechanical breakage of these fibers is modeled by addressing the structure of wildland fuel packets, the breakage mechanism of thermochemically eroding fibers, and the effect of thermal degradation on fuel properties.

2.1. Structure of wildland fuels

The typical approach for modeling branching vegetative structures in the literature is based on fractal geometry, which was first articulated by Mandelbrot [6] and has been incorporated into computational methods for generating realistic tree structures by researchers such as Collin et al. [7]. This work follows the approach of Collin et al. for modeling deciduous trees by assuming that the wildland fuel packet consists of n branching stages of cylindrical fibers of diameter D_i and length L_i, as shown in Fig. 1. It is assumed that the branching stages are self similar, so that both the diameter ratio between successive branching stages D_{i+1}/D_i and the aspect ratio $A = L_i/D_i$ are constant with respect to i. While not required for the methodology, it is assumed that each branching process is a bifurcation process, where one branch divides into exactly two smaller branches. The limbs of the tree are assumed to have no defects and are assumed to not taper, and it is assumed that the trees of interest have lost their leaves and consist of cylindrical fibers only. The geometry of leaves differs greatly from that of branches, and their behavior during thermal degradation and lofting is very different from that of branches and requires additional modeling not addressed here. There are many examples of wildfires that arise in the plains regions of the United States (e.g., in Texas) during the winter season when grasses have cured and trees have lost their leaves. As such, the assumption of leafless trees is not outrageous.

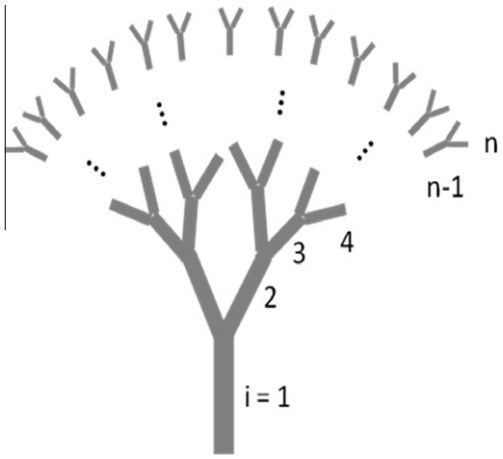

Fig. 1. Fractal model for branching vegetation wildland fuel packet.

The trajectory and life expectancy for any particular lofted brand is highly dependent upon its initial geometry. Because the available range of geometries for branching wildland fuels is vast, it is important to estimate the distribution of mass and branch sizes for a wildland fuel packet in order to assess its ember lofting potential in a wildfire scenario. The fractal self similarity assumption provides a means to determine the distribution of mass at different levels of branching within a tree. The ratio of mass, m, between two successive stages of branching is

$$\frac{m_i+1}{m_i} = \frac{\rho_s V_{i+1}}{\rho_s V_i} = \frac{\rho_s\left[n_{i+1}\left(\frac{\pi}{4}D_{i+1}^2\right)AD_{i+1}\right]}{\rho_s\left[n_i\left(\frac{\pi}{4}D_i^2\right)AD_i\right]} = \left(\frac{n_{i+1}}{n_i}\right)\left(\frac{D_{i+1}}{D_i}\right)^3 \quad (1)$$

where n_i and n_{i+1} are the number of branches in each stage, ρ_s is the solid density, V is the branch volume, and A is the aspect ratio. Mandelbrot reports that although the diameter ratio D_{i+1}/D_i varies greatly among different species of trees, a generally acceptable value is $D_{i+1}/D_i = 2^{-1/2} \approx 0.71$. Using this and the splitting ratio $n_{i+1}/n_i = 2$, one obtains

$$m_{i+1}/m_i = 2\left(2^{-\frac{1}{2}}\right)^3 = 2^{-\frac{1}{2}} \approx 0.71 \quad (2)$$

Equation (2) suggests that the amount of mass in a stage of branching decreases as the stage's nominal diameter decreases. Recall that this analysis is made for trees with no leaves and a splitting ratio of 2. With leaves, or with a different splitting ratio, one imagines that the mass scaling would be quite different.

2.2. Thermo-mechanical breakage mechanism

For cellulosic elements in a large scale fire, two thermal degradation processes may occur: pyrolysis and oxidation. During pyrolysis, volatile gasses are exhausted from the solid, leaving behind a material with a higher percentage of carbon. During this process, there is a decrease in density and strength of the element, but no significant change in its volume or shape. The oxidative degradation process can be viewed as a surface mass loss process in which material is removed from the surface of the solid, and the surface of the solid recedes with no significant changes to density or strength. Because pyrolysis generally occurs at a lower temperature than oxidation, it is assumed that pyrolysis occurs before oxidation, and breakage may occur due to either the decrease in strength associated with pyrolysis or the subsequent thinning of fibers due to oxidation. Each of these failure mechanisms is considered sequentially. Currently, the spatial and temporal evolution of strength and density for branches undergoing pyrolysis in wildfire scenarios is not well understood, and only the final post-pyrolysis density and strength are estimated in this model. These values are used to determine whether or not fracture is possible due to pyrolysis only, and if it is not, the time varying mass loss due to oxidation is modeled with post-pyrolysis properties fixed. The time varying oxidation process is the main focus of the current modeling, and expressions are now developed for mass loss of branches due to oxidation and for the critical state of stress in the branches when a breakage event occurs.

For a cylindrical branch element undergoing oxidation to reduce the diameter, the diameter D can be shown to evolve in time according to Eq. (3) when a B number model for solid combustion is used. Hilpert's [8] correlation is used for the Nusselt number, $\overline{Nu_D} = C Re_D^m Pr^{1/3}$, where C and m are functions of the Reynolds number

$$\frac{dD}{dt} = -2C\alpha_a \frac{\rho_a}{\rho_s} \ln(1+B) \left(\frac{U}{v_a}\right)^m Pr^{1/3} D^{m-1} \tag{3}$$

The thermal diffusivity, density, and kinematic viscosity of air are α_a, ρ_a, and v_a, respectively. While the branch is decomposing on the parent plant, if it is assumed that the external flow velocity U is constant, one can integrate over the oxidation time t_{ox} from the initial diameter D_o to any later diameter D_{ox}. The following expression for the diameter ratio, D_{ox}/D_o, during oxidation is obtained

$$\frac{D_{ox}}{D_o} = \left[1 - 2(2-m)\frac{\rho_a}{\rho_s} \ln(1+B)\overline{Nu_{D_o}} \left(\frac{t_{ox}}{D_o^2/\alpha_a}\right)\right]^{\frac{1}{2-m}} \tag{4}$$

While oxidizing on the parent plant, a given branch i is subjected to a variety of loads, as shown in Fig. 2. As time passes, the diameter of the branch decreases until it reaches a critical diameter D_{cr}, at which point it fractures at its attachment point to the parent and is carried into the plume. Each branch is subjected to the force of its own weight $F_{w,i}$ and a drag force $F_{d,i}$ exerted in the direction of the plume flow. It is assumed that the flow velocity is always opposite to the direction of the gravitational force, in accordance with the buoyant plume model. Additionally, each branch is subjected to bending moments and shear forces from the smaller branches $i+1$ in the subsequent stage of branching. It will be shown that these smaller branches are removed earlier than branch i, so that at the time of fracture branch i is subjected only to the force of its own weight and the drag force.

The bending moment, M, at the base of branch i is

$$M_i = \frac{L_i}{2}\cos\theta_i \left[\frac{1}{2}\rho_a U^2 C_d D_i L_i - \rho_s \frac{\pi}{4} D_i^2 L_i g\right] \tag{5}$$

where C_d is the drag coefficient. Dropping subscript i, the maximum flexural stress, σ, in the cylindrical branch subjected to M is defined and combined with Eq. (5) to obtain

$$\sigma = \frac{32M}{\pi D^3} = \frac{8L^2\cos\theta}{\pi D^2}\left[\rho_a U^2 C_d - \frac{\pi}{2}\rho_s D g\right] \tag{6}$$

Using the aspect ratio $A = L/D_o$ and rearranging gives a polynomial for D/D_o. Three-point bending tests are used to determine the critical flexural stress, σ_{cr}, for wood specimens. The diameter of a branch is said to have been reduced to a critical value, D_{cr}, when the flexural stress in the branch reaches the critical flexural stress, σ_{cr}. Incorporating this into the polynomial for D/D_o gives

$$\left(\frac{D_{cr}}{D_o}\right)^2 + 2\left(\frac{2\rho_s g D_o A^2\cos\theta}{\sigma_{cr}}\right)\left(\frac{D_{cr}}{D_o}\right) - \left(\frac{\frac{8}{\pi}\rho_a U^2 C_d A^2\cos\theta}{\sigma_{cr}}\right) = 0 \tag{7}$$

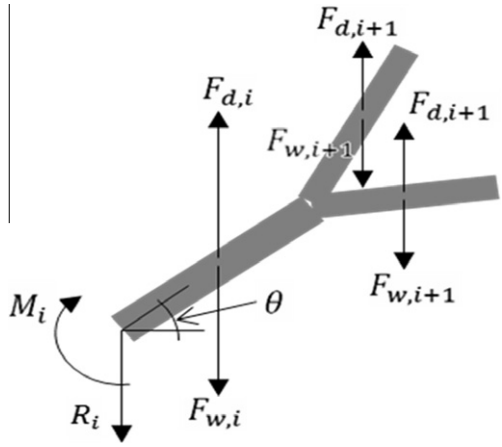

Fig. 2. Overall force distribution on branch i.

Defining $\sigma_w = 2\rho_s g D_o A^2 \cos\theta$ as the characteristic stress associated with the weight of the branch and $\sigma_d = \frac{8}{\pi}\rho_a U^2 C_d A^2 \cos\theta$ as the characteristic stress associated with drag on the branch, the failure criterion can be expressed in simple nondimensional form. The physically relevant root of this polynomial is

$$\frac{D_{cr}}{D_o} = \left[\left(\frac{\sigma_w}{\sigma_{cr}}\right)^2 + \left(\frac{\sigma_d}{\sigma_{cr}}\right)\right]^{1/2} - \left(\frac{\sigma_w}{\sigma_{cr}}\right) \tag{8}$$

It is most interesting to determine how the initial diameter of a branch affects the breakage process. It should be observed that D_o is contained only within σ_w/σ_{cr} and not within σ_d/σ_{cr}. For situations in which $\sigma_w \ll \sigma_{cr}$ or $\sigma_d/\sigma_{cr} \gg \sigma_w/\sigma_{cr}$, the dependence on initial diameter becomes negligible and the simple result $D_{cr}/D_o = (\sigma_d/\sigma_{cr})^{1/2}$ is obtained.

The expression for the time evolution of the oxidizing branch (Eq. (4)) can be nondimensionalized using σ_w to replace D_o in the right side of the equation. Representative values of $C = 0.683$ and $m = 0.5$ for the Hilpert correlation (valid for $40 < Re_D < 4000$) are used and one obtains:

$$\frac{D_{ox}}{D_o} = \left[1 - \frac{t_{ox}}{\tau}\left(\frac{\sigma_w}{\sigma_{cr}}\right)^{-3/2}\right]^{2/3}, \quad D_{ox} > D_{cr} \tag{9}$$

which is valid whenever the diameter is greater than the critical diameter; the time constant τ is

$$\tau = \left[3C\frac{\rho_a}{\rho_s}\ln(1+B)\left(\frac{U}{\nu}\right)^{1/2} Pr^{1/3}\alpha_a\left(\frac{2\rho_s g A^2\cos\theta}{\sigma_{cr}}\right)^{3/2}\right]^{-1} \tag{10}$$

A breakage event is determined by the intersection of Eqs. (8 and 9). If D_{ox}/D_o is greater than D_{cr}/D_o, then the branch remains on the plant, but when t_{ox}/τ increases to the point that $D_{ox}/D_o = D_{cr}/D_0$, then the branch fractures.

Figure 3 plots D_{ox}/D_o and D_{cr}/D_o versus σ_w/σ_{cr} for different values of t_{ox}/τ and σ_d/σ_{cr}, respectively. As previously noted, when σ_w/σ_{cr} is small, the weight of the branch is negligible and does not influence the state of stress; the value for D_{cr}/D_o becomes independent of σ_w/σ_{cr}. At the other extreme, when σ_w/σ_{cr} approaches unity, the branch is so heavy that it is nearly about to fracture from the gravitational load. However, the analysis assumes that fracture occurs when a drag-induced moment that is opposite in direction to the weight-induced moment exceeds the weight-induced moment enough to subject the branch to the critical stress. As such, the branch must be oxidized to a relatively smaller diameter ratio D_{cr}/D_o for upward fracture to occur. As t_{ox}/τ increases (oxidation time increases for a given τ), the maximum initial diameter for which fracture occurs increases. It is important to note that the maximum value of σ_w/σ_{cr} for which fracture occurs increases monotonically with oxidation time for a given

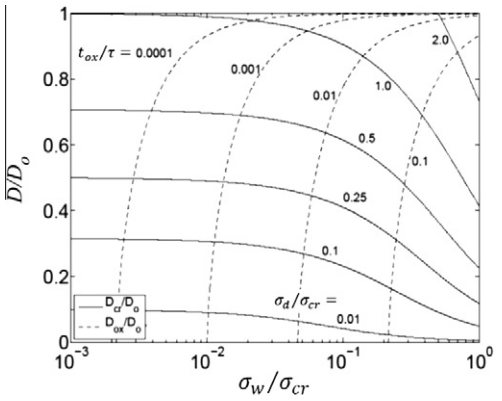

Fig. 3. D_{cr}/D_o and D_{ox}/D_o versus σ_w/σ_{cr} for different values of σ_d/σ_{cr} and t_{ox}/τ.

σ_d/σ_{cr} and τ, so small branches are always lost before large branches. This clarifies why it is reasonable to neglect the moments due to the branches in level $i + 1$ in the moment balance on branch i. Small branches oxidize faster and are broken off more frequently than large branches, which obviously agrees with observation.

2.3. Experimental characterization of pyrolyzed fuel properties

The oxidation model uses post-pyrolysis properties of fuel, namely flexural strength and solid density, as inputs. The behavior of these properties through the pyrolysis process has been studied in some detail [9], but data for specific types of wood are not widely available. A set of experiments was performed to investigate the behavior of solid density and flexural strength as a function of pyrolysis reaction progress, and the results of these tests were used to determine the appropriate post-pyrolysis data to use in the model.

The experiments performed consisted of drying and pyrolyzing sets of wooden dowel rods and testing their flexural strength using three-point bending tests. Yellow poplar (*Liriodendron tulipifera*) dowel rods of different diameters were chosen to approximate the behavior of branches in bending because their geometry is easily measured and the tolerances in their manufacture are generally good. Rods of nominal diameter 4.8 mm, 6.4 mm, and 7.9 mm were cut into pieces 20 cm long and divided into three testing groups, with an equal number of rods of each diameter in each group. The first group was tested at ambient conditions (14 °C, 90% relative humidity), the second was tested after oven-heating at 101 °C for 1 h, and the third was tested after oven-heating at 250 °C for 1 h.

Pyrolysis of yellow poplar occurs at a significant rate beginning at around 225 °C [10]. Oven-heating the second group resulted in mass loss

due to evaporation of moisture but no significant mass loss due to pyrolysis; the dried rods were visually indistinguishable from the unheated rods. Oven-heating the third group resulted in mass loss due to both evaporation and pyrolysis; visual inspection showed that the rods had begun to carbonize. Both of the heated groups displayed a very slight decrease in volume due to heating, but the overall densities of both groups decreased because of mass loss. The average initial and final densities for each group are shown in Table 1, along with the ratio of final density to initial density.

Three-point bending tests were performed on all samples. The span of the bending tests was 17.8 cm, and the critical load for fracture was measured after loading the samples from the center of the span. The results of the three-point bending tests for the three groups of rods are shown in Fig. 4. Also shown is a data point from the literature [11] for yellow poplar tested at 12% moisture content.

Despite the experimental scatter, Fig. 4 indicates a strong correlation between density and flexural strength. There is also a significant influence of heating history on density and strength, because the rods gain strength when dried (as observed by [9]) and then lose strength when pyrolyzed. The correlation between density and flexural strength is strongly linear, and the slopes of the linear fits to the three groups of experimental data points are reported in Table 1.

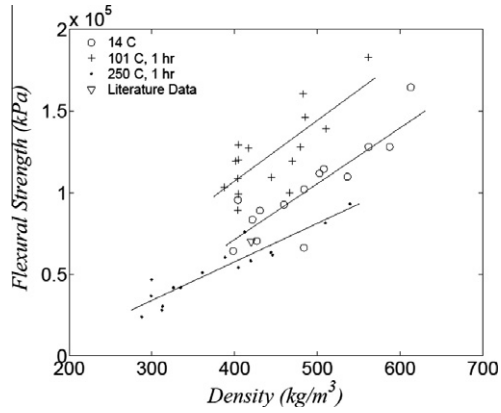

Fig. 4. Strength and density data for three-point bending tests.

3. Brand lofting model

Once the brand is removed from the tree, it travels upwards through the plume, is ejected, and drifts back to earth. The following model for brand transport was discussed by Woycheese et al. [3] and is summarized here.

While traveling through the plume and drifting to earth, the brand is subjected to its weight force, $\boldsymbol{F}_w = -mg\hat{\boldsymbol{k}}$, which acts downwards, and to a drag force, $\boldsymbol{F}_d = \frac{1}{2}\rho_a DLC_d|\boldsymbol{W}|^2\frac{\boldsymbol{W}}{|\boldsymbol{W}|}$, which acts in the direction of the relative velocity $\boldsymbol{W}$ of the external flow to the brand. Conservation of brand momentum is therefore given by $d(m\boldsymbol{V})/dt = \boldsymbol{F}_d + \boldsymbol{F}_w$, where $\boldsymbol{V}$ is the absolute velocity of the brand.

The equation of motion can be broken into horizontal and vertical velocity components V_x and V_z and simplified. The rate of change of the diameter dD/dt is given by Eq. (3), which is unchanged from the equation used for diameter change during oxidation, except that the velocity used is the relative velocity magnitude $|\boldsymbol{W}|$. The trajectory of the brands is determined from the definition of the velocity.

The relative velocity within the plume is $W_z = U_{plume} - V_z$, where U_{plume} is the absolute velocity of the air at the centerline of the plume. The plume velocity is determined using the McCaffrey plume model [12], which defines the centerline velocity as $U_{plume} = \kappa(z/\dot{Q}^{2/5})^{\eta}\dot{Q}^{1/5}$, where $\dot{Q}$ is the heat release rate of the fire. The parameters κ and η are different for each of the three regions of the plume, with the transition between regions defined by a scaled height $z/\dot{Q}^{2/5}$ [m/kW$^{2/5}$]. For the continuous flame region $z/\dot{Q}^{2/5} < 0.08$, $\kappa = 6.8$ m$^{1/2}$/s and $\eta = 1/2$, for the intermittent flame region ($0.08 < z/\dot{Q}^{2/5} < 0.2$), $\kappa = 1.9$ m/(kW$^{1/5}$ s) and $\eta = 0$, and for the plume region ($z/\dot{Q}^{2/5} > 0.2$), $\kappa = 1.1$ m$^{4/3}$/(kW$^{1/3}$ s) and $\eta = -1/3$.

After the brand exits the plume, the relative velocity in the x direction is $W_x = U_{wind} - V_x$, where U_{wind} is the absolute velocity of the prevailing ambient wind, which is assumed to be spatially uniform, and the relative velocity in the z direction is $W_z = -V_z$.

During the lofting process, the brand's diameter continues to decrease, and the length may change as it fragments into smaller pieces. The fragmentation process increases the mass loss rate of the brands because the longitudinal mass loss

Table 1
Average initial and final densities for bending specimens.

Treatment	Initial density (kg/m^3)	Final density (kg/m^3)	Density ratio	$\partial\sigma_{cr}/\partial\rho_s$ (kPa-m^3/kg)
14 °C	490	490	1.0	340
101 °C, 1 h	461	445	0.97	370
250 °C, 1 h	472	381	0.81	240

rate becomes non-negligible when the aspect ratio of the fragmenting brands becomes sufficiently small. Fragmentation effects have not been included in the present analysis because this work primarily focuses on the brand generation process.

4. Case study: Ember generation and propagation in a wildland fire

The foregoing theory is used to construct a Monte Carlo simulation for brand generation and transport in a wildland fire. The mass evolution and transport of a single brand is modeled as follows. A branch of a prescribed material with a prescribed initial diameter D_o and flexural strength σ_{cr} is pyrolyzed and oxidized in a fire with heat release rate $\dot{Q}$. It is assumed that the wildfire propagates steadily as a front, so that the branch is oxidizing within a front for a prescribed time t_{ox}. If at any point at the end of pyrolysis or during the oxidation time the diameter of the branch reaches D_{cr} (as defined by Eq. (8)), it fractures and is taken into the plume; if it does not reach D_{cr} during t_{ox}, it remains on the tree.

The lofted brands are taken into the plume and are assumed to begin their travel at the very top of the intermittent flame region. The oxidizing brands are carried upwards and ejected after some prescribed time t_{plume}. They then drift to the ground through a horizontal wind of prescribed velocity U_{wind}. If the brand returns to the ground with a diameter greater than zero, it is assumed to be of interest as a pilot to a potential spot fire.

It is assumed that the wildfire propagates over a field of trees which have the same nominal trunk diameter D_1 and the same number of branching stages n. One then wishes to determine the size of embers lofted and the size of embers deposited for the branching network with initial branch diameters $D_1, D_2, \ldots, D_n$. It is anticipated that variations in the physical parameters defining this model might affect the predictions. In particular, the branch angle of orientation θ, the plume travel time t_{plume}, and the post pyrolysis density and strength are assumed to be random. To handle these uncertainties, probability density functions are assigned to these variables and a 5000-case Monte Carlo simulation is performed for each nominal branch diameter. In the absence of detailed information about the angle of orientation for the branches, a uniform distribution is assumed between $\theta = 0$ and $\theta = \pi/2$. For t_{plume}, it is assumed that the brand will be ejected at approximately the height where the plume velocity and the prevailing wind velocity are equal, because above this point the dominant drag force is caused by the prevailing wind. The largest possible loftable brand diameter is determined for the given value of t_{ox} and the time it takes for this brand to reach the ejection point is determined. This provides an upper bound on t_{plume}, and a uniform distribution is assigned to t_{plume} between zero and this upper bound. Values for flexural strength and density are determined from the experimental characterization. It is assumed that the density of the branches is near the lower limit of the density range observed because of the wood's age, so a normal distribution with a nominal value of 290 kg/m^3 and a standard deviation of 15% is assumed for post pyrolysis density. A nominal value of 20,000 kPa is assumed for flexural strength, and strength is assumed to be proportional to density, as indicated by the linear trend of the experimental data.

The trees in the case study are assumed to be yellow poplar. The nominal trunk diameter is taken to be 8 cm, and ten branching stages are assumed, so that the nominal diameter of the smallest stage is 3.5 mm. The aspect ratio of the branches is specified to be 50 based upon measurements of tree limbs collected and analyzed for this work. Woycheese et al. report a value of 1.2 for the B number for wood burning in air, which is used here. The wildfire is assumed to have a heat release rate of 50 MW and a prevailing horizontal wind velocity of 10 m/s. The ground oxidation time t_{ox} is assumed to be 100 s, which is consistent with values reported in the literature [13]. The upper bound on the plume travel time is determined to be approximately 10 s.

The results of the Monte Carlo simulations are shown in Figs. 5 and 6. The average diameter ratios of brands lofted (D_{lofted}/D_o, equivalently D_{cr}/D_o) and deposited ($D_{deposited}/D_o$) are shown in Fig. 5, along with the analytical prediction for D_{cr}/D_o, which is obtained by setting θ to zero and using the nominal values for density and flexural strength in Eqs. (8 and 9). For a nominal oxidation time of 100 s, the maximum analytical loftable initial diameter, D_{max}, is 4.7 cm. For initial diameters above D_{max}, no value for D_{cr}/D_o can be reported, because no brands are lofted or deposited.

The lofted brand diameter ratio, (D_{lofted}/D_o, for the Monte Carlo simulations is lower than that predicted analytically for all initial diameters below D_{max}. This is because the angle of orientation θ is always greater than or equal to zero, which decreases the effective moment arm of the branch and requires more mass to be lost before fracture can occur. For initial diameters greater than D_{max}, only a small number of brands which have very low density and strength are lost, and these break with a larger diameter ratio than the analytical prediction, which is based on the nominal value for strength.

The deposited brand diameter ratio, $D_{deposited}/D_o$, for the Monte Carlo simulations is zero for the smallest branches and increases with initial diameter monotonically. This indicates that

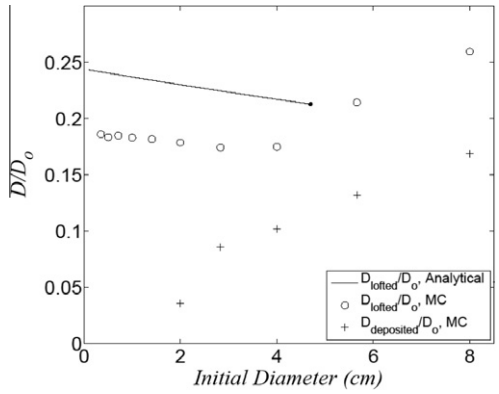

Fig. 5. Diameter ratios D_{lofted}/D_o and $D_{deposited}/D_o$ for Monte Carlo simulations, along with analytical prediction.

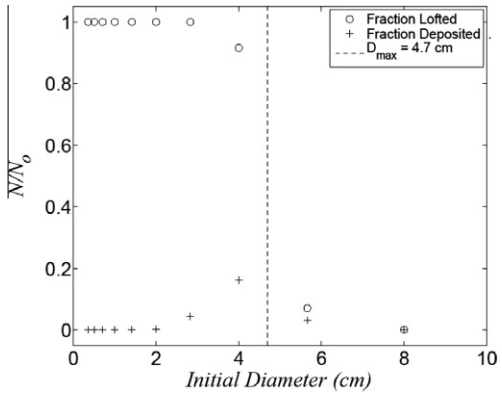

Fig. 6. Fraction by number of brands lofted and deposited.

small brands, while easily lofted, are too small to survive the lofting and propagation phases and oxidize completely in the air, while larger brands are able to survive lofting and propagation and land with appreciable mass.

Further insight is gained from Fig. 6, which shows the fraction by number, N/N_o (N_o is the original 5000 samples), of brands lofted and deposited versus initial diameter. For the initial diameters tested, all brands of initial diameter less than D_{max} are lofted (except those with very high strength), but only brands of initial diameters around 4.0 cm are deposited in appreciable numbers. Brands with very small initial diameter are easily lofted but cannot survive propagation, while brands with large initial diameters can easily survive propagation but are only very rarely lofted. The results of Figs. 5 and 6 show that there is an optimal initial diameter for brand propagation which is small enough to be lofted frequently but large enough to survive the propagation process.

The average propagation distance for brands which survive the lofting and deposition process is approximately 75 m. One notes that even for this relatively small fire (50 MW) brands are lofted and deposited over distances that might compromise structures in an urban wildland interface scenario.

The diameters of brands produced in the case study are consistent with the observations of Manzello et al. [4,5], who performed experiments on Douglas fir and collected brands with diameters on the order of 1 cm or less. The aspect ratio of the brands collected is much smaller than that used in the present study, indicating that the flexural strength of experimentally collected brands is lower than that used in the model. This discrepancy is most likely due to the difficulty of determining post pyrolysis properties of real branches based on those found experimentally. The experimentally determined values for flexural strength are found from carefully prepared specimens with uniform cross sectional area and a minimal number of defects, while branches in wildland fire scenarios have large variability in cross-sectional area, may contain numerous defects, and are wrapped in bark, whose strength properties are unknown. The dowel rods tested are also likely taken from stronger, older regions of the tree (heartwood) to provide them with additional strength, while the wood in the branch tips is younger, softer, and has lower strength (sapwood). Additionally, the heating history and post pyrolysis state of branches in a wildfire is likely different from that observed experimentally. A further investigation of the strength properties of pyrolyzed wildland fuels will be necessary to determine the appropriate values of flexural strength to use in predictive models.

It is also worth noting that the brands collected by Manzello et al. do not contain smaller elements from subsequent stages of branching. This indicates that smaller branches are indeed lost before large branches, confirming both the assumption used in determining the moment balance (Eq. (5)) and the results of Fig. 3.

5. Conclusions

A model for brand breakage for a tree with self similar branching features has been developed. The fractal property of the tree makes it possible to predict the sequence in which branches of varying diameters are lost from the tree, simplifying the moment and strength analysis for individual branches. For any individual branch the breakage model relies on aerodynamic and weight loading of branch fibers that are being oxidatively consumed. When the time-increasing stress at the branch junction equals the critical stress for the specimen, breakage occurs. The breakage model can be framed in terms of a drag-induced stress to strength ratio and weight-induced stress to

strength ratio. A limiting case is identified when the weight-induced stress to strength value is small, and one can show that a critical diameter ratio for failure is dependent only upon the drag-induced stress to strength ratio.

An experimental investigation was also performed to understand the effect of pyrolysis on the density and flexural strength of wood. The experiments showed that with heating at oven conditions, there was minimal change in sample volume, even with significant mass loss. For experimental conditions in which the wood samples were only dried, there was an increase in the flexural strength, but with subsequent heating and pyrolysis, the strength markedly decreased. The slope of the strength to final density of the wood samples was constant for a particular heating scenario. The experiments were useful in defining a reduced strength initial condition for the subsequent oxidation processes.

The breakage model was coupled to a plume and transport model taken from Woycheese et al., and a Monte Carlo wildland fire case study was performed. For wildland fires with branching fuel sources, there is an optimal branch diameter which propagates the most mass to the ground ahead of the fire front. This occurs for branches which are small enough to be removed from the tree within the time allowed by the traveling flame front but large enough to survive the transport process.

The post pyrolysis strength properties of wildland fuels have not been investigated experimentally to a significant degree. The authors hope that the present work will encourage additional work in this area as a necessary component in the development of reliable models for predicting ember generation and propagation in wildfire scenarios.

Acknowledgements

The authors acknowledge support through the Center for Predictive Engineering and Computational Science (PECOS) at the University of Texas at Austin, funded by the Department of Energy [National Nuclear Security Administration] under Award Number [DE-FC52-08NA 28615].

References

[1] F.A. Albini, *Spot Fire Distance From Burning Trees-A Predictive Model*, General Technical Report INT-56, USDA Forest Service, 1979.
[2] N. Sardoy, J.-L. Consalvi, B. Porterie, A.C. Fernandez-Pello, *Combust. Flame* 150 (2007) 151–169.
[3] J.P. Woycheese, P.J. Pagni, D. Liepmann, *J. Fire Prot. Eng.* 10 (2) (1999) 32–44.
[4] S.L. Manzello, T.G. Cleary, J.R. Shields, A. Maranghides, W. Mell, J.C. Yang, *Fire Saf. J.* 43 (2008) 226–233.
[5] S.L. Manzello, A. Maranghides, W.E. Mell, *Int. J. Wildland Fire* 16 (2007) 458–462.
[6] B.B. Mandelbrot, *The Fractal Geometry of Nature*, W.H. Freeman and Company, New York, 1977.
[7] A. Collin, A. Lamorlette, D. Bernardin, O. Séro-Guillaume, *Ecol. Model.* 222 (2011) 503–513.
[8] R. Hilpert, *Forsch. Geb. Ingenieurwes* 4 (1933) 215.
[9] B.A.-L. Ostman, *Wood Sci. Technol.* 19 (1985) 103–116.
[10] C. Vovelle, H. Mellottee, J.L. Delfau, *Kinetics of Thermal Degradation of Wood and Cellulose by T.G.A. Comparison of the Calculation Techniques*, National Meeting of the American Chemical Society, 1983.
[11] D.E. Kretschmann, *Wood Handbook, Mechanical Properties of Wood*, Department of Agriculture, Forest Service, Forest Products Laboratory, 2010 (Chapter 05).
[12] B.J. McCaffrey, *Purely Buoyant Diffusion Flames: Some Experimental Results*, NBSIR 79-1910, National Bureau of Standards, 1979.
[13] E.A. Johnson, K. Miyanishi, *Forest Fires: Behavior and Ecological Effects*, Academic Press, San Diego, 2001.